Molecular Crystals and Liquid Crystals

Publication details, including instructions for authors and subscription information:
http://www.tandfonline.com/loi/gmcl20

Dielectric Permittivity of Nematics with a Molecular Based Continuum Model

Alberta Ferrarini [a]

[a] Dipartimento di Chimica Fisica, Università di Padova, via Loredan 2, Padova, 35131, Italy

Version of record first published: 18 Oct 2010

To cite this article: Alberta Ferrarini (2003): Dielectric Permittivity of Nematics with a Molecular Based Continuum Model, Molecular Crystals and Liquid Crystals, 395:1, 233-252

To link to this article: http://dx.doi.org/10.1080/15421400390193792

Mol. Cryst. Liq. Cryst., Vol. 395, pp. [233]/63–[252]/82, 2003

ISSN 1542-1406 print/1563-5287 online
DOI: 10.1080/15421400390193792

Taylor & Francis
Taylor & Francis Group

DIELECTRIC PERMITTIVITY OF NEMATICS WITH A MOLECULAR BASED CONTINUUM MODEL

Alberta Ferrarini
Dipartimento di Chimica Fisica, Università di Padova
via Loredan 2, 35131 Padova, Italy

A theoretical model for the dielectric permittivity of nematics has been recently proposed [1], based on the atomistic representation of a probe molecule interacting with a medium which is characterised by its macroscopic properties. Electrostatic interactions are described through the classical model of a charge distribution contained in a molecular- shaped cavity embedded in an anisotropic dielectric continuum. Short-range intermolecular interactions are parameterized in terms of the anisometry of the molecular surface, which is defined according to the "rolling sphere" representation. The results obtained for the isotropic and nematic phases of 4,4′-pentyl-cyanobiphenyl and 4,4′-pentyl-cyanobicyclohexyl are reported; a good agreement with experiment appears, with a significant improvement with respect to the Maier-Meier theory.

Keywords: dielectric tensor; cavity field; reaction field; Maier-Meier theory

INTRODUCTION

Most applications of liquid crystals rely on the possibility of aligning them with electric fields, which depends on the viscoelastic and electric properties of such materials [2]. Focusing on the latter aspect, the key quantity is the dielectric anisotropy; for nematics, which are uniaxial with respect to the director, this is defined as $\Delta\varepsilon = \varepsilon_{\parallel} - \varepsilon_{\perp}$, where the symbols $\parallel$ and $\perp$ denote directions respectively parallel and perpendicular to the director. From the molecular point of view, the origin of the dielectric anisotropy is the anisotropic distribution of the molecular dipoles in the liquid crystal phases. So, nematic phases formed by elongated molecules carrying longitudinal and transverse dipoles have respectively positive and negative dielectric anisotropy, whose magnitude increases with that of the molecular dipoles and with the degree of ordering, *i.e.* with decreasing temperature.

The author acknowledges financial support from MURST *PRIN Cristalli Liquidi* and EU *TMR* contract *FMRX CT97 0121*.

A simple model for the quantitative estimate of the dielectric tensor from molecular properties was derived by Maier and Meier [3], by extending to anisotropic phases the Onsager theory for the dielectric constant [4], based on the model of a molecule as a spherical polarizable cavity with a central dipole, embedded in a dielectric medium. In the Maier-Meier theory some further assumptions are introduced, related to the molecular anisotropy which is the basis of the nematic order. Molecules are approximated as uniaxial particles which tend to align the C_∞ symmetry axis to the nematic director, whose polarizability has components $\alpha + 2\Delta\alpha/3$ and $\alpha - \Delta\alpha/3$ parallel and perpendicular to the C_∞ axis respectively. Thus, the components of the dielectric permittivity parallel and perpendicular to the nematic director can be expressed as

$$\varepsilon_{\parallel(\perp)} = 1 + \frac{NhF}{\varepsilon_0}\left[\frac{F\langle\mu^2_{0\parallel(\perp)}\rangle}{k_BT} + \langle\alpha_{\parallel(\perp)}\rangle\right], \tag{1}$$

where N is the molecular number density, and $\boldsymbol{\mu}_0$ is the permanent dipole moment of the molecule, which makes an angle θ with the C_∞ axis. The brackets in Eq. (1) denote averages over the nematic distribution function, for which the Maier-Saupe form [5] is assumed. The various terms can be expressed as:

$$\begin{aligned} &\langle\mu^2_{0,\parallel}\rangle = \mu_0^2[1 + 2P_2(\cos\theta)\langle P_2\rangle]/3 \qquad \langle\mu^2_{0,\perp}\rangle = \mu_0^2[1 - P_2(\cos\theta)\langle P_2\rangle]/3 \\ &\langle\alpha_\parallel\rangle = \alpha + (2/3)\Delta\alpha\langle P_2\rangle \qquad \langle\alpha_\perp\rangle = \alpha - (1/3)\Delta\alpha\langle P_2\rangle \end{aligned} \tag{2}$$

where P_2 is the second Legendre polynomial and $\langle P_2\rangle = \langle 3\cos^2\beta - 1\rangle/2$, with β the angle between the director and the C_∞ axis, is the orientational order parameter.

The effect of the environment in Eq. (1) is introduced through the factors h and f, which are proportionality factors respectively between (i) the applied electric field $\boldsymbol{E}_\infty$ and the field experienced in the spherical cavity (cavity field $\boldsymbol{E}_C$), and (ii) the molecular dipole and the electric field due to the polarization of the dielectric environment (reaction field $\boldsymbol{E}_R$) [6]. They are defined in the same way as for the isotropic phase:

$$h = \frac{3\varepsilon}{2\varepsilon + 1} \qquad f = \frac{1}{a^3}\frac{2\varepsilon - 2}{2\varepsilon + 1}\ , \tag{3}$$

being $\varepsilon = (\varepsilon_\parallel + 2\varepsilon_\perp)/3$ the mean dielectric permittivity and a the radius of the spherical cavity. This can be estimated through the Onsager hypothesis $4\pi a^3/3 = M/d$, being M the molar mass and d the density . The factor $F = 1/(1 - \alpha f)$ in Eq. (1) is introduced to account for polarizability effects in the reaction field. Note that in the definition of the factors h, f, F the

anisotropy of the permittivity and that of the molecular polarizability are completely neglected.

The Maier-Meier equations have been widely used to correlate the dielectric permittivity of nematics with the magnitude and direction of the molecular dipole and with the molecular polarizability, and to explain the temperature dependence of the permittivity tensor [7–9]. Lack of quantitative agreement with experiment, which often occurs, can be ascribed to the limits of the model. These can be summarized as:

- neglect of the dependence of intermolecular correlations on the specific structure of the interacting molecules, which is a general drawback of continuum approaches;
- use of simplifying approximations, *i.e.* the representation of the cavity shape and charge distribution as a sphere with a central dipole, as well as the neglect of anisotropy effects in the cavity and reaction field factors.

Only the first point is usually taken into account, and the discrepancies between theoretical and experimental data are used to estimate the degree of short-range intermolecular correlations, so implicitly assuming the small significance of the latter assumptions [7,8].

With the purpose of investigating the consequences of the neglect of the molecular features, a molecular based continuum approach has recently been developed [1]. The mean dipole moment is calculated by averaging the molecular dipole over the orientational distribution function in the nematic phase in the presence of an applied field, which is expressed in terms of a short-range contribution and a long-range electrostatic term. The latter is derived from the electrostatic free energy of the system, which is calculated with a continuum model, by considering the interaction of the charge distribution contained in the molecular cavity with both the polarization of the surrounding dielectric and the applied electric field as experienced within the cavity. The generalisation of an integral equation formalism developed in the quantum mechanical context [10] allows the detailed account of the molecular shape and charge distribution in the anisotropic phase. The molecular cavity is modelled with atomistic detail according to the Richards-Connolly representation [12] and the charge distribution is described in terms of partial charges located at the nuclear positions, in addition to induced dipoles calculated on the basis of distributed polarizabilities [13]. Also the short-range contribution to the orientational distribution function is calculated by taking into account the molecular structure, by using a phenomenological mean field, parameterized according to the anisometry of the molecular surface [14]. An analogous approach was also used to describe the effects of electrostatic interactions on orientational order of solutes in liquid crystal solvents [11].

In this work the theory will be applied to 4-*n*-pentyl-4′-cyanobiphenyl (5CB) and 4-*n*-pentyl-4′-cyanobicyclohexyl (5CCH), two compounds with a similar structure, but displaying a quite different permittivity. As will be shown, the Maier-Meier predictions strongly overestimate the dielectric permittivity, especially in the first case, but the introduction of the molecular features and a more accurate account of the dielectric anisotropy of the medium can improve the quality of the predictions of the continuum approach.

THEORY

The theory and the computational methodology have been presented in ref [1], therefore only the main points of the approach will be reported here.

Under the linear approximation, the macroscopic expression for the polarization of a dielectric is given by [15]

$$\boldsymbol{P} = \boldsymbol{\chi}\mathbf{E}_{\infty} \ , \tag{4}$$

where $\boldsymbol{\chi}$ is the (first order) dielectric susceptibily, related to the dielectric permittivity $\boldsymbol{\varepsilon}$ by the expression $\boldsymbol{\chi} = \varepsilon_0(\boldsymbol{\varepsilon} - 1)$. From a microscopic point of view, the polarization in a homogeneous phase is linked to the average electric dipole moment

$$\boldsymbol{P} = \frac{N}{V}\langle\boldsymbol{\mu}\rangle \ , \tag{5}$$

where the term within brackets is the statistical average of the molecular dipole $\boldsymbol{\mu}$.

From comparison of Eqs. (4) and (5) the following expression for the components of the (relative) dielectric permittivity tensor is obtained:

$$\varepsilon_{IJ} = \delta_{IJ} + \frac{N}{V\varepsilon_0}\frac{\partial\langle\mu_I\rangle}{\partial E_{\infty,J}} \ , \tag{6}$$

with the labels $\boldsymbol{I}$,$\boldsymbol{J}$ denoting components in the laboratory frame.

A molecular theory for the dielectric permittivity should provide expressions for the average dipole moment $\langle\boldsymbol{\mu}\rangle$ as a function of the applied field $\boldsymbol{E}_{\infty}$. By adopting the usual partition in permanent and induced charges, this can be expressed as the sum

$$\langle\boldsymbol{\mu}\rangle = \langle\boldsymbol{\mu}_0\rangle + \langle\boldsymbol{\mu}^{\mathrm{ind}}\rangle \ . \tag{7}$$

The average values are calculated as

$$\langle\cdots\rangle = \int \cdots f(\Omega)d\Omega \ , \tag{8}$$

where Ω are the Euler angles specifying the molecular orientation and $f(\Omega)$ is the single particle distribution function which, by adopting a molecular field approach is defined as

$$f(\Omega) = \frac{\exp\lfloor -U(\Omega)/k_BT \rfloor}{\int \exp\lfloor -U(\Omega)/k_BT \rfloor d\Omega} \ , \tag{9}$$

with the orientational molecular field $U(\Omega)$. This derives (i) from the coupling between the molecule and the applied field and (ii) from interactions with the surrounding molecules in the nematic phase; by denoting the two contributions respectively as $W_{C+\delta R}$ and U_0, we can write:

$$U(\Omega) = W_{C+\delta R}(\Omega) + U_0(\Omega) \ . \tag{10}$$

For sufficiently weak applied fields the power expansion of the exponential $\exp[-W_{C+\delta R}/k_BT]$ in Eq. (9) can be truncated at the linear term, so that we can approximate

$$f(\Omega) \approx f_0(\Omega)\left[1 - \frac{W_{C+\delta R}}{k_BT}\right] \ , \tag{11}$$

where $f_0(\Omega)$ represents the orientational distribution function in the nematic phase in the absence of external fields:

$$f_0(\Omega) = \frac{\exp[-U_0(\Omega)/k_BT]}{\int \exp[-U_0(\Omega)/k_BT] d\Omega} \ . \tag{12}$$

By recognising the origin of the orienting interactions, the contribution $U_0(\Omega)$ can, in turn, be decomposed as

$$U_0(\Omega) = U_{sr}(\Omega) + W_R(\Omega) \ , \tag{13}$$

with the two contributions amenable respectively to short-range interactions modulated by the molecular shape and to electrostatic-induction interactions depending on the molecular charge distribution.

In the recently developed methodology all quantities required for the calculation of the dielectric permittivity are determined from the molecular structure: the permanent dipole moment $\boldsymbol{\mu}_0$ is calculated from atomic charges, the short-range contribution to the orienting potential in the nematic phase, U_{sr}, is modelled according to the surface tensor approximation [14], while the induced dipole moment, $\boldsymbol{\mu}^{\text{ind}}$, and electrostatic free energies in the presence and in the absence of the applied field, $W_{C+\delta R}$ and W_R respectively, are obtained by a continuum dielectric approach [1].

Dielectric Continuum Model

Let us consider the charge distribution $\rho(\boldsymbol{r})$ contained in a cavity C embedded in a dielectric with permittivity $\boldsymbol{\varepsilon}$, in the presence of an applied

field $\boldsymbol{E}_\infty$, which can be thought of as due to the charge distribution ρ_∞ placed in the dielectric at infinite distance from the cavity. The electrostatic potential $V(\boldsymbol{r})$ is the solution of the differential equations [6,15]

$$\begin{cases} -\partial^2 V(\boldsymbol{r})/\partial \boldsymbol{r}^2 = \rho(\boldsymbol{r})/\varepsilon_0 & \boldsymbol{r} \in \mathcal{C}_I \\ -\partial/\partial \boldsymbol{r} \cdot \boldsymbol{\varepsilon} \cdot \partial V(\boldsymbol{r})/\partial \boldsymbol{r} = \rho_\infty/\boldsymbol{\varepsilon}_0 & \boldsymbol{r} \in \mathcal{C}_E \end{cases} \tag{14}$$

where $\mathcal{C}_I$ and $\mathcal{C}_E$ are space regions inside and outside of the cavity, with the boundary conditions on the surface S of the cavity:

$$\begin{cases} V_e(\boldsymbol{r}) - V_i(\boldsymbol{r}) = 0 & \text{on } S \\ \partial_e V(\boldsymbol{r}) - \partial_i V(\boldsymbol{r}) = 0 & \text{on } S. \end{cases} \tag{15}$$

In these equation the operators

$$\partial_i = \left(\frac{\partial}{\partial \boldsymbol{r}}\right)_i \cdot \boldsymbol{s}(\boldsymbol{r}) \quad \partial_e = \boldsymbol{\varepsilon}\left(\frac{\partial}{\partial \boldsymbol{r}}\right)_e \cdot \boldsymbol{s}(\boldsymbol{r}) \tag{16}$$

have been introduced, where $\boldsymbol{s} = \boldsymbol{s}(\boldsymbol{r})$ is a unit vector normal to the surface at $\boldsymbol{r}$ and outward pointing, and the subscripts e and i are used to denote functions respectively on the inner and outer side of the surface S.

The electrostatic potential V can be considered as the superposition of (i) the potential generated by the charge distribution $\rho(\boldsymbol{r})$ in a vacuum, and (ii) a contribution deriving from the polarization of the environment and from the applied field. The (ii) term, which can be associated with what are usually denoted respectively as the reaction and cavity fields [6], is the relevant one in the present context. It depends on the characteristic of the molecular cavity and charge distribution and on the dielectric permittivity of the surrounding fluid. It is possible to show, essentially by making use of relations derived from the Green's formula [10,1], that this contribution can be expressed as an integral which involves an apparent charge density σ on the surface of the cavity, accounting for cavity and reaction field effects. Such a charge density is the solution of the integral equation over the surface of the cavity:

$$\mathcal{A}\sigma = -g_R - g_R^{\text{ind}} - g_C \ , \tag{17}$$

with

$$\mathcal{A} = \left(\frac{\mathcal{I}}{2} - \mathcal{D}_e\right)\mathcal{S}_i + \mathcal{S}_e\left(\frac{\mathcal{I}}{2} + \mathcal{D}_i\right) \tag{18a}$$

$$\left.\begin{aligned} g_R &= \left(\mathcal{B}\varphi_i^0\right)(\boldsymbol{r}) \\ g_R^{\text{ind}} &= \left(\mathcal{B}\varphi_i^{\text{ind}}\right)(\boldsymbol{r}) \\ g_C &= \boldsymbol{E}_\infty \cdot \boldsymbol{r} \end{aligned}\right\}, \text{with } \mathcal{B} = \left(\tfrac{\mathcal{I}}{2} - \mathcal{D}_e\right) + \varepsilon_0 \mathcal{S}_e \partial_i \Bigg\} \boldsymbol{r} \in \mathcal{S}. \tag{18b}$$

In these equations $\mathcal{I}$ is the identity operator, while $\mathcal{A}$ and $\mathcal{B}$ are defined in terms of the following operators, which depend on cavity shape and dielectric permittivity of the medium:

$$\left.\begin{aligned}(\mathcal{S}_i\ h)(\boldsymbol{r}) &= \int_s G_I(\boldsymbol{r},\boldsymbol{r}')h(\boldsymbol{r}')d\boldsymbol{r}' \\ (\mathcal{D}_i\ h)(\boldsymbol{r}) &= \varepsilon_0 \int_s \boldsymbol{s}(\boldsymbol{r})\cdot\langle\partial G_I(\boldsymbol{r},\boldsymbol{r}')/\partial\boldsymbol{r}\rangle h(\boldsymbol{r}')d\boldsymbol{r}' \\ (\mathcal{S}_e\ h)(\boldsymbol{r}) &= \int_s G_E\ h(\boldsymbol{r}')d\boldsymbol{r}' \\ (\mathcal{D}_e\ h)(\boldsymbol{r}) &= \varepsilon_0 \int_s \boldsymbol{s}(\boldsymbol{r})\cdot\boldsymbol{\varepsilon}\cdot\langle\partial G_E(\boldsymbol{r},\boldsymbol{r}')/\partial\boldsymbol{r}'\rangle h(\boldsymbol{r}')d\boldsymbol{r}'\end{aligned}\right\} \quad \boldsymbol{r}\in S\ , \tag{19}$$

with the Green's functions

$$G_I(\boldsymbol{r},\boldsymbol{r}') = \frac{1}{4\pi\varepsilon_0\mid \boldsymbol{r}-\boldsymbol{r}'\mid} \tag{20}$$

$$G_E(\boldsymbol{r},\boldsymbol{r}') = \frac{1}{4\pi\varepsilon_0\sqrt{(\det\boldsymbol{\varepsilon})(\boldsymbol{r}-\boldsymbol{r}')\cdot\boldsymbol{\varepsilon}^{-1}\cdot(\boldsymbol{r}-\boldsymbol{r}')}}\ . \tag{21}$$

The functions $\varphi^0(\boldsymbol{r})$ and $\varphi^{\mathrm{ind}}(\boldsymbol{r})$ are electrostatic potentials associated, respectively, with the permanent and the induced charge distribution in the molecule, ρ^0 and ρ^{ind}:

$$\begin{aligned}\varphi^0(\boldsymbol{r}) &= \int_{R^3} G_I(\boldsymbol{r},\boldsymbol{r}')\rho^0(\boldsymbol{r}')d\boldsymbol{r}' \\ \varphi^{\mathrm{ind}}(\boldsymbol{r}) &= \int_{R^3} G_I(\boldsymbol{r},\boldsymbol{r}')\rho^{\mathrm{ind}}(\boldsymbol{r}')d\boldsymbol{r}'\ .\end{aligned} \tag{22}$$

The charge distribution ρ^0 is defined in terms of atomic charges q_K^0 located at the nuclear positions $\boldsymbol{r}_K$; then, for a molecule with N_a atoms we can write

$$\rho^0(\boldsymbol{r}) = \sum_{K=1}^{N_a} q_K^0\delta(\boldsymbol{r}-\boldsymbol{r}_K) \tag{23}$$

and

$$\varphi^0(\boldsymbol{r}) = \frac{1}{4\pi\varepsilon_0}\sum_{K=1}^{N_a}\frac{q_K^0}{\mid \boldsymbol{r}-\boldsymbol{r}_K\mid}\ . \tag{24}$$

The charge density induced in the molecule by all the fields it experiences is conveniently described in terms of local polarizabilities. Under the assumption of mutually interacting induced dipoles located at the nuclear positions, the potential $\varphi^{\mathrm{ind}}(\boldsymbol{r})$ can be written as the superposition of the potentials due to all the induced dipoles contained in the cavity:

$$\varphi^{\mathrm{ind}}(\boldsymbol{r}) = \sum_{J=1}^{N_a}\boldsymbol{t}_J(\boldsymbol{r})\cdot\boldsymbol{\mu}_J^{\mathrm{ind}} \tag{25}$$

with the vector $\boldsymbol{t}_J(\boldsymbol{r})$ defined as

$$\boldsymbol{t}_J(\boldsymbol{r}) = \frac{\boldsymbol{r} - \boldsymbol{r}_J}{4\pi\varepsilon_0 \mid \boldsymbol{r} - \boldsymbol{r}_J \mid^3} \ . \tag{26}$$

and the induced dipoles given by

$$\boldsymbol{\mu}_J^{\text{ind}} = -\sum_{K=1}^{N_a} \left[\boldsymbol{M}^{-1}\right]_{JK} \cdot \int_S \boldsymbol{t}_K(\boldsymbol{r})\sigma(\mathbf{r})d\boldsymbol{r} \ . \tag{27}$$

Here $\left[\boldsymbol{M}^{-1}\right]_{JK}$ is the 3×3 block, corresponding to Kth and Jth atoms, of the so-called relay matrix, which gives an atomic representation of the polarizability, and the dot indicates contraction over Cartesian coordinates. The supermatrix $\boldsymbol{M}$ has dimension $3N_a \times 3N_a$, and is defined as

$$\boldsymbol{M} = \begin{bmatrix} \boldsymbol{\alpha}_1^{-1} & \boldsymbol{T}_{12} & \dots & \boldsymbol{T}_{1N} \\ \boldsymbol{T}_{21} & \boldsymbol{\alpha}_2^{-1} & \dots & \boldsymbol{T}_{2N} \\ \vdots & \vdots & & \vdots \\ \boldsymbol{T}_{N1} & \boldsymbol{T}_{N2} & \dots & \boldsymbol{\alpha}_N^{-1} \end{bmatrix} \tag{28}$$

with $\boldsymbol{\alpha} = \alpha_J \boldsymbol{I}_3$, where $\boldsymbol{I}_3$ is a 3×3 unit tensor, α_J is the atomic polarizability of the Jth center and $\boldsymbol{T}_{JK}$ is the dipole field tensor [6,15], expressing the field at the Jth nuclear position due to the presence of a dipole on the Kth atom. A modified form of this tensor was proposed by Thole, by introducing a distance dependent attenuation, so avoiding divergence of the polarizability when dipoles lie too close to each other:

$$\boldsymbol{T}_{KJ}^{Thole} = \boldsymbol{T}_K^{Thole}(\boldsymbol{r}_J) = \frac{4v_{KJ}^3 - 3v_{KJ}^4}{4\pi\varepsilon_0 |\boldsymbol{r}_J - \boldsymbol{r}_K|^3}\boldsymbol{I}_3 - \frac{3v_{KJ}^4 (\boldsymbol{r}_J - \boldsymbol{r}_K) \otimes (\boldsymbol{r}_J - \boldsymbol{r}_K)}{4\pi\varepsilon_0 |\boldsymbol{r}_J - \boldsymbol{r}_K|^5} \tag{29}$$

with

$$v_{KJ} = \begin{cases} r_{KJ}/s_{KJ} & r_{KJ} < s_{KJ} \\ 1 & r_{KJ} \geq s_{KJ} \end{cases}, \tag{30}$$

where s_{KJ} is a scaling distance:

$$s_{KJ} = x(\alpha_K \alpha_J)^{1/6}, \tag{31}$$

x being a parameter related to the width of the charge density distribution. If atoms I and J are farther apart than the scaling distance, the usual form of the dipole field [6,15] is recovered. Notice that the dipole field tensors in Eq. (29) contain the dependence on the geometry of the molecular arrangement. Therefore anisotropic molecular polarizabilities are obtained in this way, with the same symmetry of the molecular structures, even though isotropic atomic polarizabilities are assumed. The molecular polarizability is obtained by contraction of the relay matrix

$$\alpha_{\eta\zeta}^{mol} = \sum_{K=1}^{N_a}\sum_{J=1}^{N_a} [\boldsymbol{M}^{-1}]_{J\eta K\zeta}. \tag{32}$$

Electrostatic Free Energy

The dielectric model described in the previous Section enables us to give the explicit form of the terms indicated as W_R and $W_{C+\delta R}$ in Eqs.(13) and (10). The former is the contribution of intermolecular electrostatic and induction interactions to the orienting molecular field in nematics and can be identified with the energy of the molecule in its own reaction field in the absence of external fields [6]

$$W_R = \frac{1}{8\pi\varepsilon_0}\sum_{K=1}^{N_a} q^0(\boldsymbol{r}_K)\varphi^R(\boldsymbol{r}_K), \tag{33}$$

where φ^R is the reaction electrostatic potential experienced in the absence of the external electric field. The term $W_{C+\delta R}$ represents the additional contribution derived from the presence of the external field and has the form of the interaction energy between the permanent charge distribution in the molecule and the effective applied field within the cavity:

$$W_{C+\partial R} = \frac{1}{4\pi\varepsilon_0}\sum_{K=1}^{N_a} q^0(\boldsymbol{r}_K)\left[\varphi^C(\boldsymbol{r}_K) + \varphi^{\delta R}(\boldsymbol{r}_K)\right], \tag{34}$$

where φ^C and $\varphi^{\delta R}$ are the electrostatic potentials associated respectively with the cavity field and the reaction field to the charge distribution induced in the molecule by the cavity field itself. It can be shown [1] that the whole electrostatic energy in the presence of an applied electric field can be expressed as

$$W = W_R + W_{C+\delta R} = \frac{1}{4\pi\varepsilon_0}\sum_{K=1}^{N_a} q^0(\boldsymbol{r}_K)\int_S \frac{\sigma'(\boldsymbol{r})}{|\boldsymbol{r}-\boldsymbol{r}_K|}\,d\boldsymbol{r} \tag{35}$$

with the charge density σ' which is obtained by solving the integral equation

$$\mathcal{A}\sigma' = -\frac{g_R}{2} - g_R^{\text{ind}} - g_C. \tag{36}$$

As a consequence of the dielectric anisotropy, the energy W depends on the orientation of the molecule in the nematic phase; such a dependence is conveniently represented in terms of Wigner rotation matrices [16]

$$W(\Omega) = \sum_{Lmn} W^{Lmn^*} D^L_{mn}(\Omega), \tag{37}$$

where the coefficients W^{Lmn} are defined as

$$W^{Lmn} = \frac{2L+1}{8\pi^2}\int W(\Omega)D^L_{mn}(\Omega)d\Omega \tag{38}$$

As a consequence of the different parity with respect to inversion of the contributions W_R and $W_{C+\delta R}$, they can be specified as

$$W^{Lmn} = \begin{cases} W_R^{Lmn} & (\text{even } L) \\ W_{C+\delta R}^{Lmn} & (\text{odd } L). \end{cases} \tag{39}$$

SURFACE TENSOR MODEL FOR SHORT-RANGE MEAN FIELD

The anisotropy of short-range interactions in nematic liquid crystals is described through the so called surface tensor approach, whereby it is parameterised on the basis of the anisotropy of the molecular surface [14]. By analogy with the anchoring free energy of macroscopic surfaces [17] it is assumed that each (infinitesimal) surface element dS of a molecule tends to orient its normal $\boldsymbol{s}$ perpendicular to the director $\boldsymbol{n}$ of the mesophase (in calamitic nematics), according to the mean field $dU_{sr} = \xi P_2(\boldsymbol{n} \cdot \boldsymbol{s}) dS$. In this expression P_2 is the second Legendre polynomial and ξ is a parameter (positive in calamitic nematics) expressing the orienting strength. The overall molecular field acting on a molecule is then obtained by integrating these elementary contributions over the whole molecular surface

$$U_{sr}(\Omega) = \xi \int_S P_2(\boldsymbol{n} \cdot \boldsymbol{s}) d\boldsymbol{r}. \tag{40}$$

The dependence of the molecular field on the molecular orientation can be made explicit by using the addition theorem for spherical harmonics [16]:

$$U_{sr}(\Omega) = -\xi \sum_m T^{2,m^*} D^2_{0m}(\Omega), \tag{41}$$

where $D^2_{0m}(\Omega)$ are Wigner matrix elements whose argument Ω are the Euler angles from the laboratory to the molecular frame, and $T^{2,m}$ are irreducible spherical components of a traceless second-rank tensor called the surface tensor

$$T^{2,m} = -\int_S D^{2^*}_{m0}(\Omega_s) d\boldsymbol{r}, \tag{42}$$

with the Euler angles Ω_s defining the rotation bringing the molecular $\boldsymbol{z}$ axis parallel to the surface normal $\boldsymbol{s}$.

The temperature dependence of the molecular field potential, Eqs. (41) or (42), is implicit in the orienting strength ξ. This can be assumed to be a

function of the order parameters, in the same form of the Maier-Saupe theory, generalized to biaxial particles, [18] *i.e.*

$$U_{MS}(\Omega) = -\xi_0(\lambda)T^{NI}\left(\left\langle D^2_{00}\right\rangle_0 + 2\lambda\mathcal{R}e\left\langle D^2_{02}\right\rangle_0\right)\left\{D^2_{00}(\Omega) + 2\lambda\mathcal{R}e\left[D^2_{02}(\Omega)\right]\right\}, \tag{43}$$

where $\lambda = T^{22}/T^{20}$ represents the biaxiality of the molecular field. Here $\xi_0(\lambda)$ is a constant which only depends on the biaxiality and $\langle D^2_{00}\rangle_0, \langle D^2_{02}\rangle_0$ are orientational order parameters, which for a given temperature can be found by minimizing the Helmholtz free energy of the system. Thus, for a given value of the biaxiality λ, the order parameters are unique functions of the reduced temperature $T^* = T/T_{NI}$. Comparison of Eq. (43) and Eq. (41), the latter with the surface tensor expressed in its principal axis system, leads to the expression defining the temperature dependence of the orienting strength:

$$\xi = \xi_0(\lambda)T_{NI}\left(\left\langle D^2_{00}\right\rangle_0 + 2\lambda Re\left\langle D^2_{02}\right\rangle_0\right)/T^{20}. \tag{44}$$

Actually, in our case the situation is slightly different because the total orienting potential $U_0(\Omega)$ in Eq. (13) contains, in addition to the short-range contribution modeled according to the surface tensor approach, also the electrostatic contribution $W_R(\Omega)$. However, since the latter contribution is generally much smaller than the former, the temperature dependence of the parameter ξ can still be approximated by Eq. (44).

Expressions for the Dielectric Permittivity

By using the irreducible spherical tensor notation [16], the components of the permanent dipole in the laboratory frame are related to those in the molecular frame as

$$\left(\mu_0\right)^{1p}_{\mathrm{LAB}} = \sum_q D^{1^*}_{pq}(\Omega)\left(\mu_0\right)^{1q}_{\mathrm{mol}}. \tag{45}$$

The total induced dipole moment μ^{ind} is calculated as the sum of the dipoles induced at all atomic positions, Eq. (27)

$$\boldsymbol{\mu}^{\mathrm{ind}} = \sum_{J=1}^{\mathrm{N_\alpha}} \mu^{\mathrm{ind}}_J = -\sum_{J=1}^{\mathrm{N_\alpha}}\sum_{K=1}^{\mathrm{N_\alpha}}\left[\mathbf{M}^{-1}\right]_{JK}\cdot\int_S \boldsymbol{t}_K(\boldsymbol{r})\sigma(\boldsymbol{r})d\boldsymbol{r}. \tag{46}$$

It depends on the orientation of the molecule with respect to the electric field, and again the angular dependence is conveniently represented in

terms of Wigner rotation matrices [16]

$$\mu_\varsigma^{\text{ind}} = \sum_{Lmn} (\mu_\varsigma^{\text{ind}})^{L^*_{mn}} D^L_{mn}(\Omega), \tag{47}$$

where $(\mu_\varsigma^{\text{ind}})$ is the ζ Cartesian component, in the laboratory frame, of the induced dipole and

$$(\mu_\varsigma^{\text{ind}})^{Lmn} = -\frac{2L+1}{8\pi^2} \int \mu_\varsigma^{\text{ind}}(\Omega) D^L_{mn}(\Omega) d\Omega. \tag{48}$$

Once again, we can recognize two contributions to the induced dipole moment μ^{ind}, deriving from the reaction field $\boldsymbol{E}^R$ to the molecular charge distribution, and from the effective cavity field $\boldsymbol{E}^{C+\delta R}$, proportional to $\boldsymbol{E}_\infty$. In view of the different symmetry properties of the two contributions we can write

$$\left(\mu_\varsigma^{\text{ind}}\right)^{Lmn} = \begin{cases} \left(\mu_\varsigma^{\text{ind},C+\delta R}\right)^{Lmn} & (\text{even } L) \\ \left(\mu_\varsigma^{\text{ind},R}\right)^{Lmn} & (\text{odd } L) \end{cases}. \tag{49}$$

By averaging the dipole moment over the orientational distribution function in the absence of the applied field, $f_0(\Omega)$, we obtain:

$$\left\langle \left(\mu_0\right)^{1p}_{\text{LAB}} \right\rangle_0 = -\frac{1}{k_B T} \sum_{L(\text{odd})\text{n}} W^{\text{Lpn}^*}_{C+\delta R} \sum_{q=-1}^{1} (-)^p \left(\mu_0\right)^{1q^*}_{\text{mol}} \sum_{J(\text{even})} \left\langle D^J_{0,q+n} \right\rangle_0 \times C(L,1,J;p,-p,0) C(L,1,J;q,n,n+q) \tag{50}$$

and

$$\left\langle \mu_\varsigma^{\text{ind}} \right\rangle_0 = \sum_{L(\text{even})n} (\mu_\varsigma^{\text{ind},C+\delta R})^{L0n^*} \left\langle D^L_{0n} \right\rangle_0 - \frac{1}{k_B T} \sum_{L(\text{odd})mn} W^{Lmn^*}_{C+\delta R} \times \sum_{L'n'} (\mu_\varsigma^{\text{ind},R})^{L'\underline{m}n'^*} \sum_{J(\text{even})} C(L,L',J;m,-m,0) \times C(L,L',J;n,n',n+n') \left\langle D^J_{0,n+n'} \right\rangle_0. \tag{51}$$

In writing these expressions we have assumed that the Z axis of the laboratory frame is along the C_∞ symmetry axis of the phase (in the absence of the applied field) and the axial symmetry of the phase has been exploited; therefore the following relations hold for the order parameters:

$$\left\langle D^L_{mn} \right\rangle_0 = \begin{cases} 0 & (\text{odd L}) \\ \left\langle D^L_{0n} \right\rangle_0 \delta_{m0} & (\text{even L}). \end{cases} \tag{52}$$

The expressions for the two principal components of the dielectric permittivity, $\varepsilon_{\|}$ and $\varepsilon_{\perp}$, are obtained by considering respectively the cases of an applied electric field parallel and perpendicular to the director.

(i) $\boldsymbol{E}\|\boldsymbol{n}$. The system has $C_{\infty h}$ symmetry and

$$W^{Lmn} = \begin{cases} W_{C+\delta R}^{L,0,n}\delta_{m,0} & (\text{odd } L) \\ W_{R}^{L,0,n}\delta_{m,0} & (\text{even } L) \end{cases} \tag{53a}$$

$$\left(\mu_Z^{\text{ind}}\right)^{Lmn} = \begin{cases} \left(\mu_Z^{\text{ind},C+\delta R}\right)^{L0n}\delta_{m,0} & (\text{even } L) \\ \left(\mu_Z^{\text{ind},R}\right)^{L0n}\delta_{m,0} & (\text{odd } L). \end{cases} \tag{53b}$$

Therefore the parallel component of the permittivity

$$\varepsilon_{\|} = 1 + \frac{N}{V\varepsilon_0}\frac{\partial\langle\mu_Z\rangle_0}{\partial E_\infty} \tag{54}$$

can be expressed as

$$\begin{aligned} \varepsilon_{\|} = 1 + \frac{N}{V\varepsilon_0}\Bigg\{ & \sum_{L(\text{even})n} \frac{\partial(\mu_Z^{\text{ind},C+\delta R})^{L0n^*}}{\partial E}\left\langle D_{0n}^{L}\right\rangle_0 \\ & - \frac{1}{k_B T}\sum_{L(\text{odd})\text{n}} \frac{\partial W_{C+\delta R}^{L0n^*}}{\partial E_\infty} \sum_{L'(\text{odd})n'} \left[(\mu_Z^{\text{ind},R})^{L'0n'^*} + \left(\mu_0\right)_{\text{mol}}^{1n'*}\delta_{L',1}\right] \\ & \times \sum_{J(\text{even})} C(L,L',J;0,0,0)C(L,L',J;n,n',n+n')\left\langle D_{0,n+n'}^{J}\right\rangle_0 \Bigg\}. \end{aligned} \tag{55}$$

(ii) $\boldsymbol{E} \perp \boldsymbol{n}$. If the applied field $\boldsymbol{E}$ is taken parallel to the X axis of the laboratory frame, the system has C_{2v} symmetry and

$$W^{Lmn} = \begin{cases} W_{C+\delta R}^{L,\pm1,n}\delta_{m,\pm1} & (\text{odd } L) \\ W_{R}^{L,0,n}\delta_{m,0} & (\text{even } L) \end{cases} \tag{56a}$$

$$\left(\mu_X^{\text{ind}}\right)^{Lmn} = \begin{cases} \left(\mu_X^{\text{ind},C+\delta R}\right)^{Lmn} & (\text{even } L, \text{even } m) \\ \left(\mu_X^{\text{ind},R}\right)^{L\pm1n}\delta_{m,\pm1} & (\text{odd } L). \end{cases} \tag{56b}$$

The perpendicular component of the dielectric permittivity can be expressed as

$$\varepsilon_{\perp} = \varepsilon_X = 1 + \frac{N}{V\varepsilon_0}\frac{\partial\langle\mu_X\rangle_0}{\partial E_\infty} \tag{57}$$

and, by recalling that

$$\mu_X = \frac{-\mu^{11} + \mu^{1-1}}{\sqrt{2}} = -\sqrt{2}\mathcal{R}e\mu^{11} \tag{58}$$

we can write

$$\begin{aligned}\varepsilon_\perp =& 1 + \frac{N}{V\varepsilon_0}\left\{ \sum_{L(\text{even})n} \frac{\partial(\mu_X^{\text{ind},C+\delta R})^{L0n^*}}{\partial E_\infty} \left\langle D^L_{0n} \right\rangle_0 \right. \\ & - \frac{1}{k_B T} \sum_{L(\text{odd}),n} \sum_{L'(\text{odd})n'} \left[\frac{\partial W^{L1n^*}_{C+\delta R}}{\partial E_\infty} (\mu_X^{\text{ind},R})^{L'\underline{1}n'^*} + \frac{\partial W^{L\underline{1}n^*}_{C+\delta R}}{\partial E_\infty} (\mu_X^{\text{ind},R})^{L'1n'^*} \right. \\ & \left. \left. + \frac{1}{\sqrt{2}} \left(\frac{\partial W^{L,1,n^*}_{C+\delta R}}{\partial E_\infty} - \frac{\partial W^{L,\underline{1},n^*}_{C+\delta R}}{\partial E_\infty} \right) (\mu_0)^{1n'^*}_{mol} \delta_{L',1} \right] \right. \\ & \left. \times \sum_{J(even)} C(1, L, J; -1, 1, 0) C(1, L, J; n', n, n+n') \left\langle D^J_{0,n'+n} \right\rangle_0 \right\}. \end{aligned} \tag{59}$$

Equations (55) and (59) are self-consistency equations for the dielectric tensor. If only the first contribution is considered, the high frequency components of the permittivity tensor, $\varepsilon_{\infty\parallel}$ and $\varepsilon_{\infty\perp}$, are obtained. It can be seen that, with some further approximations, *i.e.* spherical cavity shape, molecular charge assimilated to an ideal central dipole and Maier-Saupe orientational distribution, the Maier-Meier relations are recovered [1].

RESULTS AND DISCUSSION

Calculations have been performed for 4-*n*-pentyl-4′-cyanobiphenyl (5CB) and 4-pentyl-4′-cyanobicyclohexyl (CCH5), by considering in both cases only the all-*trans* conformers, which have the highest statistical weight. Geometry optimisation has been performed with *ab-initio* methodology at the HF/6-31G* level [19] and partial charges have been obtained with the Merz-Kollman-Singh procedure [20]. Molecular structures and charges are shown in Figure 1, together with the calculated and experimental values of the permanent dipole moments, μ_0. For both molecules the molecular dipole moment is nearly parallel to the CN bond. As usually occurs, the quantum mechanical calculations overestimate the dipole moments; the measured values [21] are roughly 80% of the theoretical prediction. Therefore, in our calculations, reduced charges have been used, scaled in such a way as to reproduce the measured dipole moments. The molecular surface, used for the definition of the molecular cavity in the electrostatic

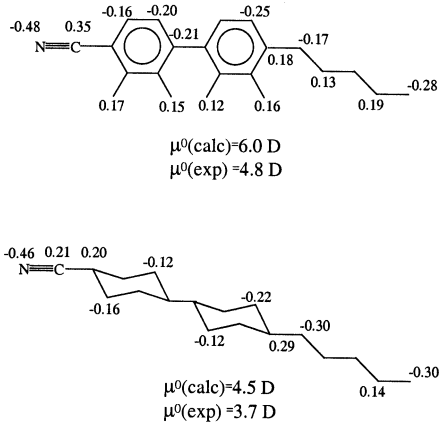

FIGURE 1 Structure of 5CB (upper) and CCH5 (lower), with the partial charges larger than 0.1 (a.u.). The calculated and experimental [21] dipole moments are also reported.

problem and for the evaluation of the surface tensor, has been calculated with the rolling sphere algorithm, in the implementation given by Spehner *et al*. [22], by using the following van der Waals radii: $r_C = 1.85$ Å, $r_N = 1.6$ Å, $r_H = 1.2$ Å for aliphatic hydrogens and $r_H = 1$ Å for aromatic hydrogens, together with a rolling sphere radius equal to 3 Å and a triangle density of 5 vertices Å^{-2}. Polarizability effects have been introduced through the Thole model of smeared interacting induced dipoles, with the parameterization proposed in ref. [23]. The molecular polarizabilities obtained in this way are reported in Table I. For both molecules the average value is close to the

TABLE I Calculated and Experimental Values of the Polarizability (Molecular Components, Average, and Anisotropy $\Delta\alpha = \alpha_{zz} - (\alpha_{xx+}\alpha_{yy})/2)$. The $\{x, y, z\}$ Axes are Shown in Figure 2

Molecule	α_{xx}/Å^3	α_{yy}/Å^3	α_{zz}/Å^3	α/Å^3	$\Delta\alpha$/Å^3
5CB					
calc	20.4	26.0	46.9	31.1	23.7
exp [24]				33.2	23.9
exp [21]				33.8	17.5
CCH5					
calc	25.3	29.5	49.7	34.8	22.3
exp [25]				36.9	6.5
exp [21]				32.0	11.4

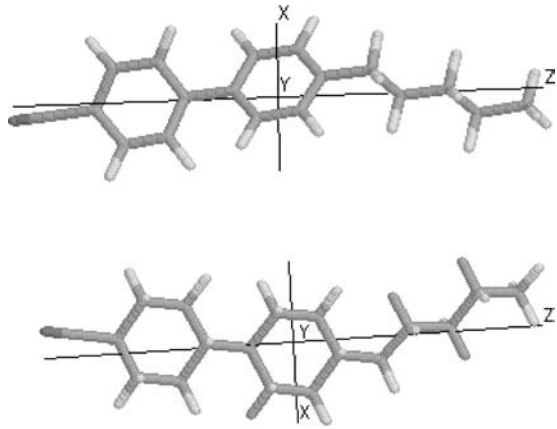

FIGURE 2 Optimized geometries of 5CB (upper) and CCH5 (lower). The molecular frames, with the {x, y, z} axes along the principal axes of the polarizability tensors, are shown.

experimental one, but the anisotropy $\Delta\alpha$, which is rather well reproduced for 5CB, appears to be overestimated for CCH5.

The surface tensors of 5CB and CCH5 are very similar, as could be expected in view of the close shape similarity of the two compounds; this means that a similar orienting behaviour is predicted in the two cases. The principal axes of the surface tensor, as well as those of the Saupe matrix $\boldsymbol{S}$, are roughly parallel to the $\{x, y, z\}$ axes shown in Figure 2.

The dielectric permittivities calculated for the isotropic phase of 5CB and CCH5 are reported in Table II, while the temperature dependence of the principal components of the permittivity tensor predicted for the two systems in the nematic phase are shown in Figures 3 and 4. For both the isotropic and the nematic phase we also report experimental values and those calculated with the Onsager and Maier-Meier relations, respectively.

TABLE II Nematic-Isotropic Transition Temperature, Density and Dielectric Constant in the Isotropic Phase of 5CB and CCH5. The Last Two Columns Report the Dielectric Permittivity in the Isotropic Phase Predicted by the Present Method and the Onsager Theory, Respectively

Molecule	T_{NI}/K	D/g cm^{-1}	ε (exp)	ε (calc)	ε (calc.- O)
5CB	308.5	$1.002^{313K}_{[26]}$	$11.2^{311K}_{[27]}$	11.2	18.2
CCH5	358.4	$0.881^{363K}_{[25]}$	$7.3^{363K}_{[25]}$	6.5	8.6
			$6.0^{363K}_{[28]}$		

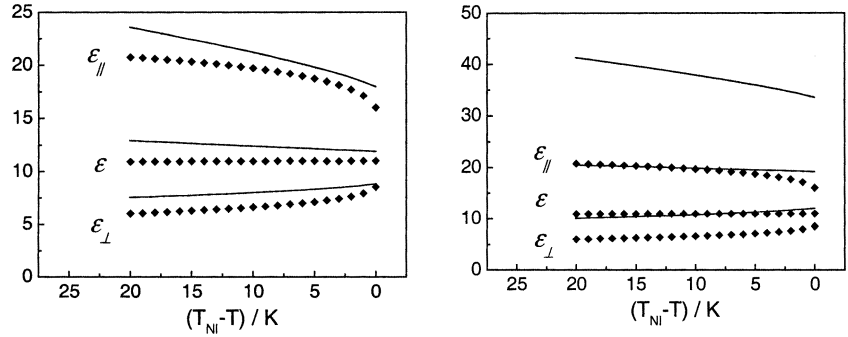

FIGURE 3 Principal components and average value of the dielectric permittivity tensor of 5CB as a function of the shifted temperature from the nematic-isotropic transition. Theoretical: solid line (left: present model, right: Maier-Meier theory). Experimental: diamonds [27].

Such calculations have been performed by using in Eqs. (1)–(2) the experimental dipole moment, μ_0, and for the average polarizability, α, and polarizability anisotropy, $\Delta\alpha$, the values reported in Table I. The angle θ between dipole moment and main orientational axis in the molecule has been taken equal to 0° for 5CB and 15° for CCH5.

A large amount of experimental data are available for 5CB; in Table I and in Figure 3 we have reported those recently obtained with accurate measurements by Faetti and Bogi [27], which anyway are not very

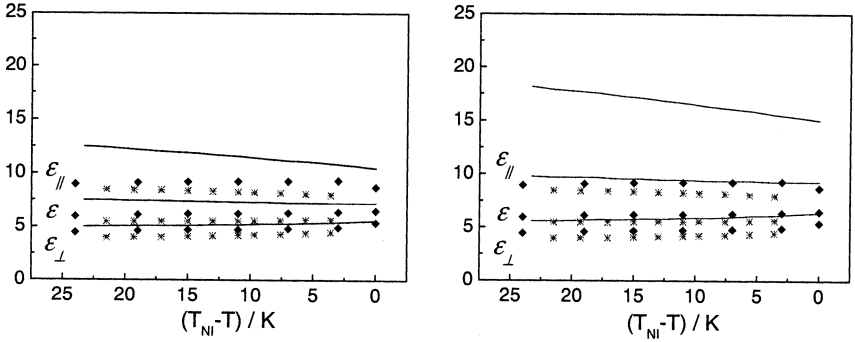

FIGURE 4 Principal components and average value of the dielectric permittivity tensor of CCH5 as a function of the shifted temperature from the nematic-isotropic transition. Theoretical: solid line (left: present model, right: Maier-Meier theory). Experimental: diamonds [25] and asterisks [28].

different from those previously presented by other authors [29]. We can see that the dielectric constant predicted by our model for 5CB in the isotropic phase is in perfect agreement with the experimental result, and also the theoretical values of the dielectric tensor in the nematic phase are close to the measured ones. Actually, a closer agreement of the latter could hardly be expected, in view of the many factors affecting this property. Namely, even in the presence of a theoretical description allowing for a completely satisfactory prediction of the dielectric constant of the liquid, the quality of the results for nematics is not ensured, in view of the role played in this phase by orientational order, which needs to be modeled in a suitable way. Moreover it is possible that molecular details, like the anisotropy of the molecular polarizability, can be more critical when dealing with anisotropic properties. Certainly the difference between the measured and theoretical slope of the curves $\varepsilon_{//}/\varepsilon_{\perp}$ *vs* T, which can be seen in Figure 3 and is particularly strong close to the nematic-isotropic transition, derives from the approximate modelling of the molecular order. However, it should be remarked that the prediction of the temperature dependence of orientational order with this level of accuracy would require very sophisticated treatments, taking into account effects as director fluctuations and coupling between order and thermodynamic variables [30]. In view of all this, we can be quite satisfied with the results shown in Figure 3. The quality of the theoretical predictions can be appreciated even more if they are compared with those of the Onsager and Maier-Meier theories, which are affected by errors of the order of 100%.

As could easily be expected from the lower dipole moment, the dielectric permittivity predicted for CCH5 is substantially lower than for 5CB. In this case the comparison with experiment is not so straightforward, because of the scarcity of experimental data in the literature and their poor consistency. Namely, in one case a rather uncommon behaviour is reported, with the dielectric anisotropy decreasing with decreasing temperature [28], while in another the usual temperature dependence is displayed [25]. We can see from Table II that the permittivity predicted for liquid CCH5 lies between the two sets of reported data, while Figure 4 shows that the theoretical values of the components of the dielectric tensor in the nematic phase are larger than both the experimental ones. Anyway, the discrepancies between theoretical and experimental data do not exceed 20% and they are significantly lower than those resulting from the Onsager and Maier-Meier theories for the isotropic and the nematic phase, respectively. As appears from comparison of Figures 3 and 4, the overestimation increases with the magnitude of the the molecular dipole. In contrast, the differences between experimental values and predictions of the present approach are comparable for 5CB and CCH5. Probably they reflect the

intrinsic limits of the methodology and better predictions can hardly be expected; besides the difficulty, mentioned previously, of accurately modelling the orientational order, we should recall the approximations related with the representation of the molecular cavity and the definition of partial charges and molecular polarizabilities.

CONCLUSION

The dielectric permittivities of the isotropic and nematic phases of 5CB and CCH5 have been predicted by using a recently developed continuum approach, which can be viewed as an extension of the Onsager and Maier-Meier theories, for isotropic liquids and for nematics respectively, enabling specific account of the molecular structure to be taken. The method combines the reaction-cavity field approximations for the electrostatic interactions and the surface tensor modelling of the anisotropy of the short-range interactions. The relevant molecular properties are the molecular surface and the charge distribution, which is represented in terms of partial charges and mutually induced dipoles, located at the nuclear positions. The two compounds investigated in the present work, 5CB and CCH5, have similar structures, but quite different bulk dielectric properties. Their dielectric permittivities exhibit large deviations from the predictions of the Onsager theory in the isotropic phase, and even larger are those from the Maier-Meier theory in the nematic; the dielectric permittivity is overestimated for both compounds, and the effect is particularly pronounced in the case of the strongly polar 5CB. Our calculations have shown that even in the context of continuum models good agreement with experiment can be obtained, provided that the structure of the molecule is suitably taken into account. Among the various factors, the cavity anisometry seems to be the most relevant; as reported elsewhere [1], the improvement with respect to the predictions of the Onsager theory becomes substantial as the molecular shape gets less globular. Also the replacement of the point dipole with a realistic charge distribution is important; however, as long as the partial charges have reasonable values, small variations of them have been seen to have no dramatic effects. In this work a single all-*trans* conformation was taken for 5CB and CCH5; however this should not be a major restriction, since calculations performed for some other conformers led to similar results. Finally, it has to be recalled that the method presented here suffers the drawbacks of continuum approaches, and this has to be taken into account in assessing its predictions: dipole correlations are somehow contained in it, but the short-range contributions, which depend on the structure of the neighbouring molecules, are completely absent. Various manifestations of the latter in liquid

crystals have been claimed; the present calculations suggest that their role might be less dramatic than what can be estimated on the basis of over-simplified approaches.

REFERENCES

[1] di Matteo, A. & Ferrarini, A. (2002). *J. Chem. Phys.*, *117*, 2397.
[2] Vertogen, G. & de Jeu, W. H. (1988). *The Physics of Liquid Crystals, Fundamentals*, Springer, Berlin.
[3] Maier, W. & Meier, G. (1961). *Z. Naturforsch. A*, *16*, 262; *ibidem*, *16*, 470 (1961).
[4] Onsager, L. (1936). *J. Am. Chem. Soc.*, *58*, 1486.
[5] Maier, W. & Saupe, A. (1959). *Z. Naturforsch. A, 14*, 882; *ibidem*, *15*, 287, (1960).
[6] Böttcher, C. J. F. & Bordewijk, P. (1973). *Theory of Electric Polarization*, Elsevier, Amsterdam.
[7] Dunmur, D. & Toriyama, K. (1998). *In Handbook of Liquid Crystals, Vol. 1 Fundamentals*, Demus, D., Goodby, J., Gray, G. W., Spiess, H.-W., & Vill, V. (Eds.), Wiley-VCH, Weinheim.
[8] Urban, S. (2001). *In Physical Properties of Liquid Crystals:Nematics*, Dunmur, D. A., Fukuda, A., & Luckhurst, G. R. (Eds.), INSPEC, London.
[9] Kresse, H. (1982). *Fortsch. der Physik*, *30*, 507.
[10] Cancès, E. & Mennucci, B. (1998). *J. Math. Chem.*, *23*, 309; Mennucci, B., Cancès, E., & Tomasi, J. (1997). *J. Phys. Chem. B*, *101*, 10506.
[11] di Matteo, A., Ferrarini, A., & Moro, G. J. (2000). *J. Phys. Chem. B*, *104*, 7764; di Matteo, A., & Ferrarini, A. (2001). *ibidem*, *105*, 2837.
[12] Richards, F. M. (1977). *Ann. Rev. Biophys. Bioeng.*, *151*, 6; Connolly, M. L. (1983). *J. Appl. Cryst.*, 16, 548.
[13] Thole, B. T. (1981). *Chem. Phys.*, *59*, 341.
[14] Ferrarini, A., Moro, G. J., Nordio, P. L., & Luckhurst, G. R. (1992). *Mol. Phys.*, 77, 1; Ferrarini, A., Janssen, F. Moro, G. J., & Nordio, P. L. (1999). *Liq. Crystals*, *26*, 201.
[15] Jackson, J. D. (1975). *Classical Electrodynamics*, 2nd ed. (Wiley, New York).
[16] Zare, N. R. (1987). *Angular Momentum*, Wiley, New York.
[17] Rapini, A. & Papoular, M. (1969). *J. Phys.* (*Paris*) *Colloq.*, *30C4*, 54.
[18] Luckhurst, G. R., Zannoni, C., Nordio, P. L., & Segre, U. (1975). *Mol. Phys.*, *30*, 1345.
[19] Frisch, M. J. et al. (1998). *Gaussian 98* (*Revision A.6*), Gaussian Inc., Pittsburgh PA.
[20] Besler, B. H., Merz, K. M., & Kollman, P. A. (1990). *J. Comp. Chem.*, *11*, 431; Singh, U. C., & Kollman, P. A. (1984). *J. Comp. Chem.*, *5*, 129.
[21] Dunmur, D. A. & Tomes, A. (1983). *Molec. Cryst. Liq. Cryst.*, *97*, 241.
[22] Sanner, M. F., Spehner, J.-C., & Olson, A. J. (1996). *Biopolymers*, *38*, 305.
[23] van Duijnen, P.Th. & Swart, M. (1998). *Phys. Chem. A*, *102*, 2399.
[24] Baran, J. W., Borowski, F., Kedzierski, J., Raszewski, Z., Zmija, J., & Sadowska, K. W. (1978). *Bull. Pol. Acad. Sci.*, *25*, 117.
[25] Sen, S., Kali, K., & Roy, S. K. (1988). *Bull. Chem. Soc. Japn.*, *61*, 3681.
[26] Karat, P. P. & Madhusudana, N. V. (1977). *Mol. Cryst. Liq. Cryst.*, *40*, 239.
[27] Bogi, A. & Faetti, S. (2001). *Liq. Crystals*, *28*, 729.
[28] Bradshaw, M. J. & Raynes, E. P. (1981). *Molec. Cryst. Liq. Cryst.* (*Letters*), *72*, 35.
[29] Jadžin, J., Czerkas, S., Czechowski, G., Burczyk, A., & Dabrowski, A. (1999). *Liq.Crystals*, *3*, 437; Cummins, P. G., Dunmur, D. A., & Laidler, D. A. (1975). *Mol. Cryst. Liq. Cryst.*, *30*, 109; Ratna, B. R. & Shashidar, R. (1977). *Mol. Cryst. Liq. Cryst.*, *42*, 185; Jadzin, J., & Kedziora, P. (1987). *Mol. Cryst. Liq. Cryst.*, *145*, 17.
[30] Ferrarini, A., & Moro, G. J. (2001). *J. Chem. Phys.*, *114*, 596.